Effect of Particle Size on Colloidal Solid Triglycerides

ARTICLE *in* LANGMUIR · MAY 2000

Impact Factor: 4.46 · DOI: 10.1021/la990856l

Articles

Effect of Particle Size on Colloidal Solid Triglycerides

Heike Bunjes,*,† Michel H. J. Koch,‡ and Kirsten Westesen†

Department of Pharmaceutical Technology, Institute of Pharmacy, Friedrich Schiller University Jena, Lessingstrasse 8, 07743 Jena, Germany, and European Molecular Biology Laboratory, Hamburg Outstation, EMBL c/o DESY, Notkestrasse 85, 22603 Hamburg, Germany

Received July 1, 1999. In Final Form: February 24, 2000

The size-dependent behavior of different crystalline, colloidal monoacid and complex triglycerides in aqueous dispersion is investigated, mainly by differential scanning calorimetry and X-ray diffraction. With decreasing particle size the melting range of the triglycerides broadens and shifts to lower temperatures. The melting of particles in small-size dispersions (e.g., with mean particle sizes around 100 nm) of even, saturated monoacid triglycerides such as tripalmitin and trimyristin is characterized by a sequence of discrete sharp transitions which are not due to polymorphism. This complex melting process is observed with different types of stabilizers. The sequence of melting events originates from the shape and layered structure of the triglyceride nanocrystals leading to successive discrete transitions corresponding to the melting of particle fractions with different thickness. In dispersions of complex triglycerides, the individual transitions are less sharp or even undetectable. The heat of fusion and the crystallization temperature of the nanoparticles decrease slightly with decreasing particle size whereas the rate of polymorphic transitions increases. Moreover, dispersions containing extremely small nanoparticles display an X-ray diffraction pattern indicating the presence of a crystal form that seems not to have been described previously for these triglycerides.

Introduction

Aqueous suspensions of triglyceride nanoparticles are under investigation as novel drug carrier systems, e.g., for intravenous administration.[1] Such dispersions can be obtained by emulsification of molten triglycerides in a hot aqueous phase using adequate stabilizers. Upon cooling, the emulsified glycerides recrystallize to form suspensions of particles. The preparation of solid nanoparticles in the lower colloidal size range (e.g., smaller than 100−150 nm) may, for several reasons, be advantageous for pharmaceutical applications. Variations of the particle size within the colloidal range may, however, affect some of the physicochemical properties of the nanoparticles. It has been shown earlier that the behavior of colloidally dispersed triglycerides differs significantly from that of their bulk phases, e.g., in terms of recrystallization temperature and time course of polymorphic transitions.[2−4] The aim of the present study was to investigate the influence of particle size on the melting and crystallization behavior as well as on the polymorphic transitions of triglyceride nanoparticles. Beyond the technological aspects, investigations on the structure and behavior of nanoparticles from crystalline organic substances are of broader interest since such particles have hitherto been studied in far less detail than their inorganic counterparts.

This study concentrates on tripalmitin and trimyristin suspensions stabilized with the nonionic surfactant tyloxapol. Additional investigations on differently stabilized tripalmitin dispersions were performed to check for stabilizer effects. The influence of the matrix material was studied by comparison with results from other simple triglycerides (trilaurin, tristearin) and complex triglyceride mixtures.

Materials

The triglycerides Dynasan 112 (trilaurin, D12), 114 (trimyristin, D14), 116 (tripalmitin, D16), and 118 (tristearin, D18) were provided by Hüls AG (D-Witten). The purity of the fatty acid fraction is approximately 95% for D14 and D16 and 99% for D12 and D18. The hydroxyl value (quantity (mg) of potassium hydroxide required to neutralize the acid combined by acylation in 1 g of the substance) as an indication for free hydroxyl groups due to the presence of partial glycerides is below 5 in all cases. Witepsol H 42 (H42) and Softisan 154 (S154), also from Hüls AG, are complex triglyceride mixtures with a fatty acid fraction consisting of approximately 44% C12, 15% C14, 23% C16, and 16% C18 (H42), or 49% C16 and 46% C18 (S154) beside minor amounts of shorter and longer chain fatty acids. The maximum hydroxyl value of H42 is 3, and that of S154 is 10 (triglyceride data according to manufacturer's specifications). The following materials were obtained from the indicated sources and used without further purification: Soya lecithin Lipoid S100 (Lipoid KG, D-Ludwigshafen), sodium glycocholate (Sigma, St. Louis), Tyloxapol USP (Sterling Organics, Rensselaer), thiomersal (Synopharm, D-Barsbüttel), glycerol 85% (Wasserfuhr, D-Bonn), and bidistilled water.

Methods

Sample Preparation. The triglycerides were melted, and if applicable, the phospholipids were dispersed in the melt by ultrasonication until an optically clear liquid was obtained. The

* Telephone: ++49 3641 949903. Fax: ++49 3641 949902. E-mail: Heike.Bunjes@rz.uni-jena.de.
† Friedrich Schiller University Jena.
‡ European Molecular Biology Laboratory.

(1) Westesen, K.; Siekmann, B. In *Microencapsulation*; Benita, S., Ed.; Marcel Dekker: New York, 1996; pp 213−258.
(2) Westesen, K.; Siekmann, B.; Koch, M. H. J. *Int. J. Pharm.* **1993**, *93*, 189−199.
(3) Siekmann, B.; Westesen, K. *Colloids Surf. B* **1994**, *3*, 159−175.
(4) Bunjes, H.; Westesen, K.; Koch, M. H. J. *Int. J. Pharm.* **1996**, *129*, 159−173.

10.1021/la990856l CCC: $19.00
Published on Web 05/19/2000

Table 1. Preparation and PCS Particle Size Parameters of the Dispersions

code[a]	matrix material	stabilizer	homogen. press. [bar]	temp. [°C]	*z*-aver. [nm]/PI
D16-Ty-490	10% D16	1.5% Tyl	300	80	492/0.22[b]
D16-Ty-260	10% D16	1.5% Tyl	500	80	261/0.21
D16-Ty-210	10% D16	3% Tyl	300	80	210/0.20
D16-Ty-165	10% D16	3% Tyl	800	80	164/0.19
D16-Ty-160	10% D16	3% Tyl	800	80	160/0.18[c]
D16-Ty-180	10% D16	3% Tyl	800	80	182/0.14
D16-Ty-95	10% D16	6% Tyl	1200	80	93/0.20
D16-Ty-100	10% D16	6% Tyl	1200	80	98/0.20[c]
D16-Ty-100	10% D16	6% Tyl	1200	80	101/0.18
D16-Ty-65	10% D16	10% Tyl	1500	80	63/0.20[c]
D16-Ty-65	10% D16	10% Tyl	1500	80	66/0.19
D14-Ty-365	10% D14	1.5% Tyl	300	70	366/0.27[b]
D14-Ty-160	10% D14	3% Tyl	800	70	160/0.19
D14-Ty-100	10% D14	6% Tyl	1200	70	99/0.20
D14-Ty-65	10% D14	10% Tyl	1500	70	66/0.21
D12-Ty-100	10% D12	6% Tyl	1200	65	102/0.23[d,e]
D18-Ty-110	10% D18	6% Tyl	1200	85	111/0.20[d]
H42-Ty-410	10% H42	1.5% Tyl	300	60	409/0.25[c]
H42-Ty-160	10% H42	3% Tyl	800	60	162/0.26[c]
H42-Ty-110	10% H42	6% Tyl	1200	60	110/0.22[c]
H42-Ty-65	10% H42	10% Tyl	1500	60	63/0.23[c]
S154-Ty-225	10% S154	3% Tyl	300	85	227/0.25
S154-Ty-100	10% S154	6% Tyl	1200	85	101/0.20
D16-PT-335	10% D16	1.25% S100, 1.25% Tyl	500	75	337/0.23[b]
D16-PT-165	10% D16	2.5% S100, 2.5% Tyl	1000	75	165/0.23
D16-PG-205	10% D16	2.4% S100, 0.6% SGc	600	80	204/0.15
D16-PG-135	10% D16	3.2% S100, 0.8% SGc	1200	80	134/0.19
D16-PG-110	10% D16	4% S100, 1% SGc	1500	80	111/0.20[c]

[a] D18, D16, D14, D12: Dynasan 118, 116, 114, 112. H42: Witepsol H42. S154: Softisan S154. Tyl: tyloxapol. S100: Lipoid S100. SGc: sodium glycocholate. temp.: preparation temperature. PI: polydispersity index. [b] Tendency toward (reversible) gel formation. If not otherwise specified, particle size analysis was performed within 1 week after preparation. [c] ≤1 month after preparation. [d] ≤6 months after preparation. [e] Emulsion particles. Sample names in italics denote dispersions which were investigated in X-ray heating scans.

hot aqueous phase (containing hydrophilic surfactants, 0.01% thiomersal as a preservative, and 2.25% glycerol to adjust tonicity) was added, and a predispersion was prepared by probe sonication in the heat. The predispersion was passed through a heated high-pressure homogenizer (Micron Lab 40, APV Gaulin, D-Lübeck) for five cycles. Dispersions with different mean particle sizes were obtained by variation of stabilizer concentration and homogenization pressure (Table 1). If possible, the dispersions were filtered (0.2 μm, in some cases 0.45 μm), and the samples were allowed to cool to room temperature. Experimental data were usually obtained on cold stored (about 4−8 °C) dispersions which, in some cases, had been brought to room temperature for some time to facilitate polymorphic transitions. Trilaurin nanoparticles do not solidify under these conditions[4] and have to be cooled to subzero temperatures to induce crystallization. Sample names follow the convention "matrix material−stabilizer composition−approximate particle size (nm)" (Table 1). Dispersions with extremely small particles were obtained by ultracentrifugation (Optima XL 80, Beckman Instruments, D-München; rotor SW 55 Ti; appr. 85 000*g*) of small-size colloidal tripalmitin and trimyristin dispersions previously diluted with the emulsifier-free aqueous phase to a triglyceride content of 2 or 3% (Table 2). Tripalmitin dispersions were centrifuged as suspensions, whereas trimyristin dispersions were centrifuged prior to crystallization of the nanoparticles. After centrifugation, the centrifuge tubes were sliced approximately 3 cm above the bottom (trimyristin) or below the meniscus (tripalmitin). The sub- (trimyristin) or supernatant (tripalmitin), respectively, was further processed. Fractions from several tubes were merged, trimyristin nanoparticles were forced to crystallize by cold storage, and a fraction of the ultracentrifugates was concentrated by ultrafiltration (stirred cell, PLTK membrane, Millipore, D-Eschborn). Ultracentrifuged samples are marked by the term "UC" followed by the duration of centrifugation in hours.

Table 2. Parameters of Ultracentrifuged Dispersions

native dispersion	centrifug. time [h]	centrifug. dispersion	*z*-average [nm]/PI
D14-Ty-100	6	D14-Ty-100-UC6	32/0.09
D14-Ty-65	18	D14-Ty-65-UC18	nd[a]
D14-Ty-65	30	D14-Ty-65-UC30	24/0.07
D16-Ty-65	4	D16-Ty-65-UC4	38/0.18
D16-Ty-65	8	D16-Ty-65-UC8	34/0.11

[a] nd: not determined.

Photon Correlation Spectroscopy (PCS). An estimate of the mean particle size was obtained by PCS at 90° (BI Zetaplus, Brookhaven Instruments Corporation, Holtsville; Zetasizer 3, Malvern Instruments, D-Herrsching). The dispersions were diluted with demineralized, filtered water to an appropriate scattering intensity. The mean particle size was approximated as the effective (*z*-average) diameter and the width of the distribution by the polydispersity index (PI) obtained by the cumulants method assuming spherical particle shape.

Differential Scanning Calorimetry (DSC). Samples were investigated in a DSC 2, DSC 7 (Perkin-Elmer, D-Überlingen) or a Micro DSC III (Setaram, F-Caluire) at different scan rates. The sample weight for the dispersions was around 10−20 mg (DSC 2, 7) or up to about 750 mg (Micro DSC III). If appropriate, dispersion samples were precooled in the DSC prior to investigation to ensure crystallization (e.g., D12) and recording of the whole melting transition. The quantity of triglyceride bulk samples was adjusted to approximately the same amount as present in the dispersion volumes used for the analysis. In some cases, bulk samples were dispersed in a tyloxapol-containing aqueous phase prior to investigation. Crystallization temperatures are given as the peak onset, and melting temperatures are given as the peak maximum temperature. The heat of fusion for the dispersed triglycerides should be regarded as approximate since the not entirely quantitative preparation technique may lead to slight variations in sample composition.

Synchrotron Radiation X-ray Diffraction. Measurements were performed on the double-focusing monochromator mirror camera X33[5] of the EMBL in HASYLAB on the storage ring DORIS III of the Deutsches Elektronen Synchrotron (DESY) at Hamburg, Germany. Two linear delay line readout detectors were connected in series to simultaneously monitor the small- and wide-angle diffraction patterns[6] using standard data acquisition and evaluation systems.[7,8] Data reduction was done following standard procedures[9] using the program SAPOKO.[10] Sample cells were thermostatized with a water bath (Huber Ministat) controlled by an IF232 programmable interface. The scattering pattern of the particles was recorded at 20 °C in at least three separate 1 min time frames to check for beam stability and radiation damage. The scattering of water was subtracted from the diffraction pattern of the dispersions. The melting behavior of native dispersions was investigated by heating the samples at 0.1 °C/min and recording the scattering pattern every minute. The diffractograms were corrected for the scattering of water, in some cases also for the diffuse scattering developing during the melting process, and the reflections of interest were integrated.

(5) Koch, M. H. J.; Bordas, J. *Nucl. Instrum. Methods* **1983**, *208*, 461−469.
(6) Rapp, G.; Gabriel, A.; Dosière, M.; Koch, M. H. J. *Nucl. Instrum. Methods A* **1995**, *357*, 178−182.
(7) Boulin, C.; Kempf, R.; Koch, M. H. J.; McLaughlin, S. M. *Nucl. Instrum. Methods A* **1986**, *249*, 399−407.
(8) Boulin, C. J.; Gabriel, A.; Koch, M. H. J. *Nucl. Instrum. Methods Phys. Res. A* **1988**, *269*, 312−320.
(9) Koch, M. H. J. In *Handbook on Synchrotron Radiation*; Ebashi, S., Koch, M. H. J., Rubenstein, E., Eds.; Elsevier: Amsterdam, 1991; pp 461−469.
(10) Svergun, D.; Koch, M. H. J.; unpublished.

After smoothing, the derivative of the resulting intensity−temperature curves was calculated. Because of their low scattering intensity, the ultracentrifugates were investigated in stepwise heating programs (the measurement temperatures approximately corresponding to the minima of the DSC curve of the ultracentifugate). For recrystallization studies, the nanoparticles were kept around 20−25 °C above their melting temperature for at least 10 min and then rapidly cooled to at least 5 °C above the onset of crystallization. Further cooling was performed at 0.3125 °C/min, and the scattering pattern was monitored continuously in 1 min time frames. The wide-angle diffractograms corrected for the scattering of water were integrated in the region of the α-reflection (around 0.415 nm), and the resulting values were normalized on the scattering of the molten triglyceride particles (intensity at the start of the measurement) to obtain the intensity−temperature correlations.

Transmission Electron Microscopy of Freeze-Fractured Specimens (FF-TEM). Samples were freeze-fractured (BAF 400, BAF 060, Bal-Tec, FL-Balzers) after fast freezing as a thin film in liquid propane or melting nitrogen. Shadowing was performed with platinum/carbon at 45°, and replica were stabilized by vertical deposition of pure carbon. After being cleaned, replica were viewed in a transmission electron microscope (EM-300, Philips, D-Kassel; CEM 902A, EM 906, Zeiss, D-Oberkochen).

Cryoelectron Microscopy. A drop of diluted dispersion was placed on an uncoated copper grid, and excess liquid was removed with a piece of filter paper. The sample was cryo-fixed by shooting into nitrogen-cooled liquid ethane. Excess ethane was removed. The sample was transferred with a cryo-transfer unit into a precooled cryoelectron microscope (CEM 902A, Zeiss, Oberkochen) operating at 80 kV with a beam current around 1 μA. Samples were viewed under low-dose conditions at a constant temperature around 80 K. For the determination of particle thicknesses, calibration was performed with catalase.

Results

Particle Size and Macroscopic Appearance of the Dispersions. The mean PCS particle size decreases with increasing emulsifier/triglyceride ratio and homogenization pressure (Table 1). Ultracentrifugation yields the small-size fractions of the dispersions (Table 2), but the concentrated ultracentrifugates tend to settle, probably due to flocculation. With other samples, at most slight to moderate sedimentation is observed upon long-term storage, and sediments can usually be redispersed easily. Some samples stabilized with a very low amount of emulsifier tend to form semisolid systems upon cold storage after preparation but reliquefy upon storage at room temperature (Table 1).

Differential Scanning Calorimetry. The melting behavior of the nanoparticles strongly depends on particle size. Particles in coarser dispersions of monoacid triglycerides melt in a single transition with a maximum slightly below that of the bulk material. With decreasing particle size, the melting transition broadens and shifts to lower temperatures. In addition, the dispersions start to display several distinct melting maxima (Figures 1−3). Melting of very finely dispersed monoacid triglycerides is thus not a continuous but a stepwise process. The particle size effect is not limited to dispersions stabilized with tyloxapol but also occurs in the D16-PT and D16-PG series. Within a series of dispersions containing the same matrix material and type of stabilizer but differing in mean particle size, the single melting maxima often appear at approximately the same temperature, albeit with different relative intensities. Very fine D14 dispersions display a broad, but distinct pretransition between about 30 and 38 °C (Figure 1). Corresponding D16 dispersions also exhibit a usually more diffuse transition at comparatively low temperatures which often passes directly into the main melting transition.

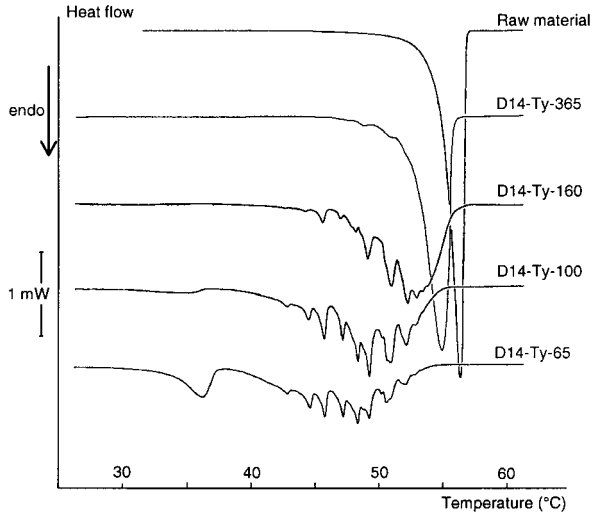

Figure 1. DSC melting curves of D14 dispersions (Micro DSC III; 0.04 °C/min). The curves are displaced along the ordinate. The raw material was dispersed in an aqueous phase containing 1% tyloxapol.

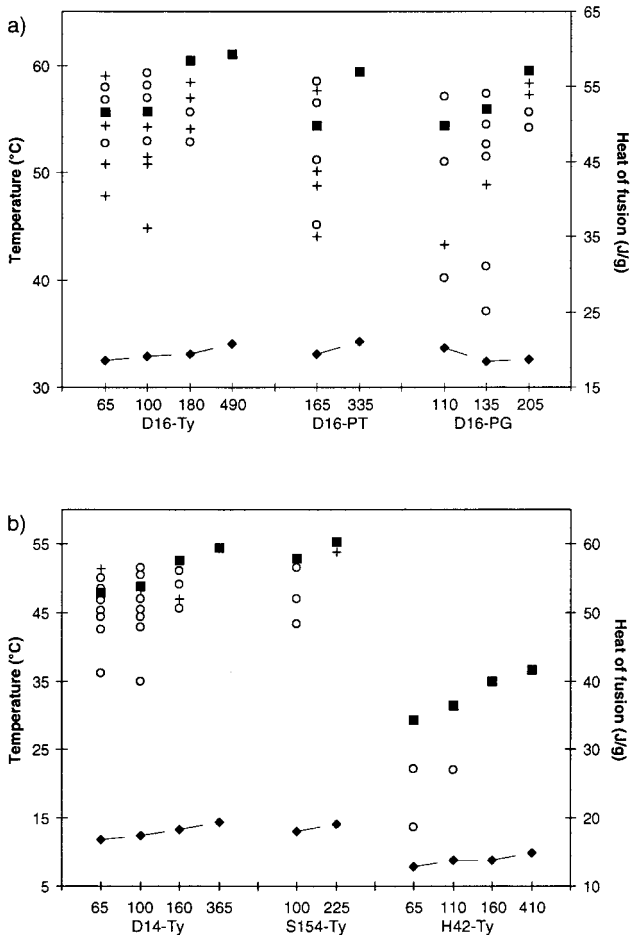

Figure 2. Melting diagrams (DSC 7; 2.5 °C/min, T_{Peak}) of D16 (a), D14, S154, and H42 dispersions (b) stored for several months (D16-PG: ca. 2 years). Transition temperatures: ■: highest peak; ○: additional maximum; +: shoulder. Heat of fusion: -◆-.

A size-dependent shift of the melting transition to lower temperatures is also detected for dispersions of complex triglycerides (Figure 2). The sample S154-Ty-100 still displays several distinct maxima, although the number of transitions is smaller than that for dispersions of monoacid triglycerides and the maxima are less sharp (Figure 3). H42 dispersions exhibit a comparatively

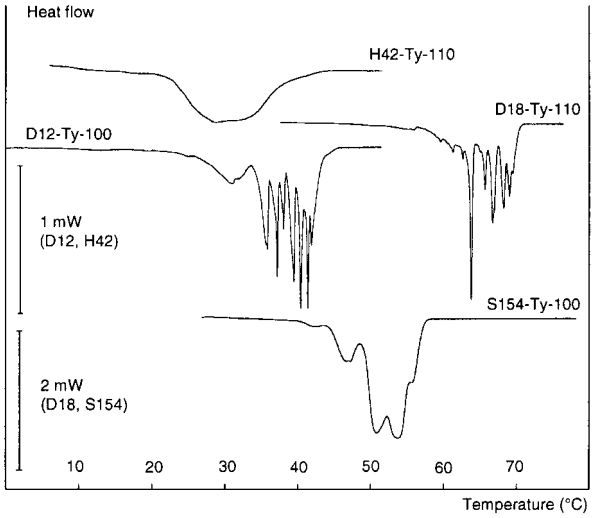

Figure 3. DSC melting curves of small-size dispersions with different matrix materials. The curves are displaced along the ordinate.

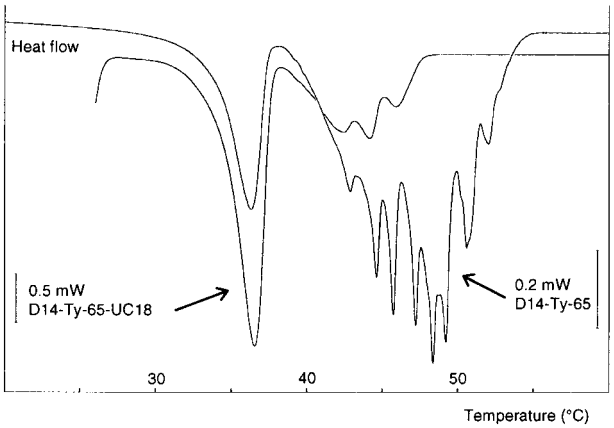

Figure 4. DSC melting curves (Micro DSC III) of the native dispersion D14-Ty-65 (0.04 °C/min) and the concentrated ultracentrifugate (18 h, 0.2 °C/min).

continuous, broad melting transition (Figure 3). In small-size H42 dispersions, additional, broad thermal events are detected at lower temperatures. Since melting starts already around or even below 10−15 °C in H42 dispersions, the transition processes of components melting below room temperature cannot be recorded without the risk of artifacts arising from melting upon sample preparation and subsequent recrystallization in the instrument.

The melting enthalpy usually decreases slightly with particle size (Figure 2).

With increasing centrifugation time, i.e., with decreasing particle size, the melting transition of the ultracentrifugates also shifts to lower temperatures (Figure 4). The relative intensity of transitions at lower temperatures increases, whereas peaks at higher temperatures become smaller and may even disappear completely. From D14 and D16 systems, the structures causing the broad pretransition between 30 and 38 °C or the diffuse transition at the beginning of the melting event, respectively, are obtained with increasing centrifugation time.

In contrast to melting, recrystallization occurs in a single, usually unstructured event. The crystallization temperatures are distinctly below those of the melting transition (e.g., between 22−25 °C for D16 and around 12−13 °C for D14 dispersions at a scan rate of 0.31 °C/min) and decrease slightly with particle size (less than 2 °C within a given series of dispersions stabilized with the same type of emulsifier but differing in particle size).

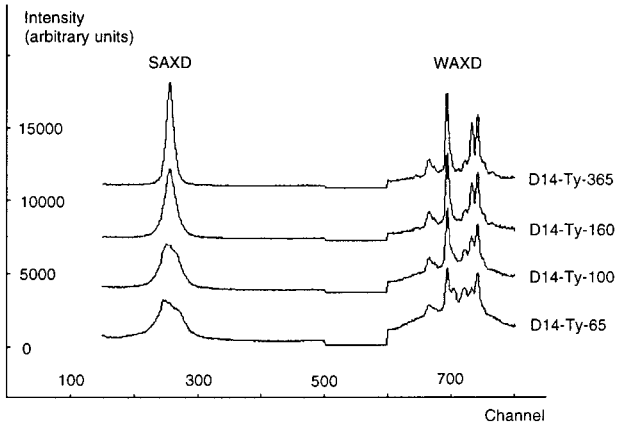

Figure 5. Small (SAXD)- and wide-angle X-ray diffractograms (WAXD) of D14 dispersions. The curves are displaced along the ordinate.

For the sample D16-Ty-95, the recrystallization behavior after incomplete melting was studied by stopping the heating run at a certain temperature during the course of the melting process. Upon subsequent cooling, crystallization starts only when the critical crystallization temperature for emulsified tripalmitin is reached. The ratio between recrystallization and melting enthalpy found for the interrupted process (0.93) corresponds to that of a complete melting and recrystallization cycle (0.94).

X-ray Diffraction. The native dispersions display wide-angle reflections around 0.46, 0.385, and 0.37 nm typical of the stable β-form of triglycerides (Figure 5). Only H42-Ty-410 still contains obvious residues of the metastable β'-modification at the time of the measurement. In general, reflections of the H42 dispersions are less sharp than those of other dispersions, and the reflection around 0.385 nm is often not being displayed distinctly.

With decreasing particle size, two additional, broad reflections around 0.44 and 0.40−0.41 nm appear in the wide-angle diffractogram of most dispersion series (Figure 5). In the sample H42-Ty-65, their intensity even approaches that of the remaining β-reflections. These reflections do not occur or have lower relative intensity in the bulk and in coarser dispersions. The small-angle reflections broaden and their maxima usually tend to shift toward lower angles with decreasing particle size. For the small-angle reflections displayed by small-size dispersions, a peak shoulder at larger angles or an asymmetry are often detected.

The additional wide-angle reflections characteristic of finely dispersed systems become more prominent in ultracentrifugates with increasing centrifugation time. Products from long-time centrifugation of lower-size dispersions which retain only particles with mean sizes around 20−30 nm display three broad main wide-angle reflections around 0.44, 0.41, and 0.37 nm (Figure 6). With exception of D14-Ty-65-UC30, an additional weak reflection around 0.46 nm, probably resulting from residues of larger particles, is detected in these dispersions. The symmetry of the very broad small-angle reflection increases with centrifugation time. Its maximum approximately corresponds to that of the original dispersion.

To correlate the stepwise melting events observed in DSC with structural characteristics of the dispersions, selected D14 and D16 dispersions (Table 1) were inves-

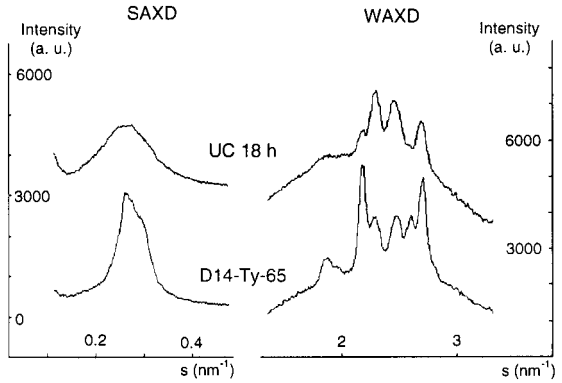

Figure 6. X-ray diffractograms of a D14 dispersion and of its concentrated ultracentrifugate: $s = 1/d = 2 \sin \Theta/\lambda$; 2Θ, scattering angle; λ, wavelength (0.15 nm). The curves are displaced along the ordinate.

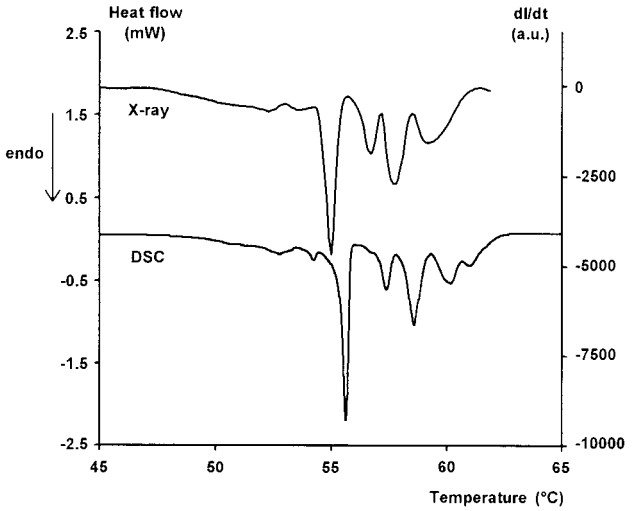

Figure 7. Comparison of DSC melting curve (Micro DSC III; 0.02 °C/min) and the change in small-angle X-ray reflection intensity (0.1 °C/min) of D16-Ty-100.

tigated in continuous heating scans. Analysis of the changes in small-angle reflection intensity of dispersions which display complex DSC thermograms also leads to curves indicating a stepwise melting transition. In many cases, the course of the DSC curve can be approximated qualitatively by the small-angle X-ray intensity curve. A comparable analysis of the wide-angle reflection intensities also often results in a curve with a shape similar to that of the DSC heating curve. A very good correlation between the DSC and small-angle reflection intensity curves is observed for D16-Ty-100 (Figure 7). Some small-angle reflection intensity curves are, however, more structured than the DSC curves, sometimes with deflections over the zero-line. The cause for this behavior could not be determined yet. A comparatively low resolution of the scattering intensity−temperature curve and the necessity to smooth this curve may contribute to this unexpected phenomenon, but alterations within the sample during the experiment may also play a role. A pronounced temporary increase in integral small-angle reflection intensity observed during melting of D16-Ty-65 might, e.g., result from recrystallization, other reorganization or agglomeration processes.

Upon melting, the width of the small-angle reflection of most dispersions decreases. In small-size dispersions, a slight shift of the peak maximum to larger angles can also be observed (Figure 8). The intensity of the pronounced

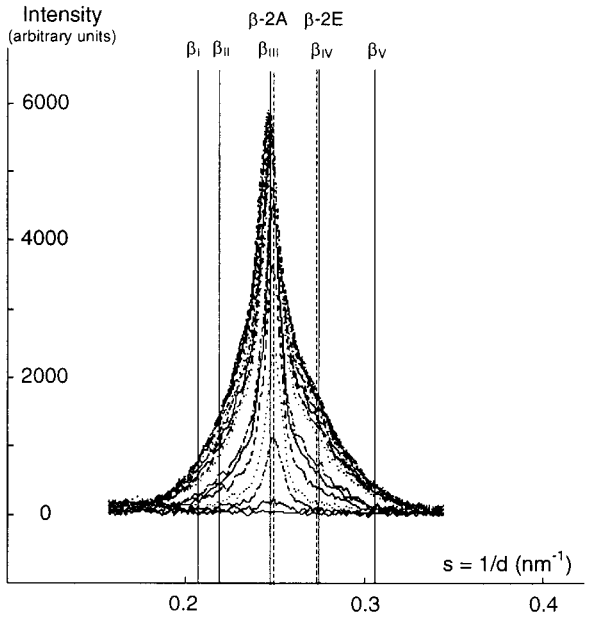

Figure 8. Evolution of the small-angle X-ray reflections of D16-Ty-100 during the melting process (temperature range: 45−62 °C). Curves are given in 1 °C steps (outer curves correspond to lower temperatures, inner to higher temperatures). In addition, reflection positions for β-submodifications after Frede and Precht[24] (—, experimental values except for β_{IV}) and de Jong and van Soest[25] (- - -) are given.

additional wide-angle reflections often observed in small-size dispersions decreases at lower temperatures than that of the characteristic β-reflections. The additional reflection around 0.44 nm usually vanishes already at comparatively low temperatures, which in the case of D14 dispersions correspond to those of the DSC pretransition. The reflection around 0.40−0.41 nm is often observed until the end of the melting process albeit with a reduced intensity. The two reflections also disappear from the diffractograms of the ultracentrifugates at temperatures in the range of the DSC pre-endotherm (D14) or the diffuse onset of melting (D16) of the systems. The intensity of the reflection around 0.46 nm present in most of the ultracentrifugates virtually does not change at low temperatures but vanishes when the temperature reaches the end-region of the corresponding DSC curve. In some cases, the reflection around 0.37 nm is also still detectable at higher temperatures.

The size dependence of polymorphic transitions after recrystallization was investigated for dispersions from the D16-Ty and D16-PG series. Crystallization proceeds via the α-modification in all dispersions, and the rate of transition into the stable β-form increases with decreasing particle size (Figure 9). The transition is slower in the D16-PG series than in the D16-Ty series, and the difference in transition rate between particles with different mean sizes is more pronounced for PG-stabilized dispersions.

Transmission Electron Microscopy. Freeze-fracture electron microscopy of the D16-Ty-165 dispersion reveals the plateletlike shape and layered structure characteristic of tripalmitin nanoparticles (Figure 10). Cryoelectron micrographs give an even better picture of the particle shape. The low contrast of platelets oriented parallel to the plane of observation suggests the existence of very thin particles. The thickness of small particles which can be obtained from platelets oriented perpendicular to the plane of observation is so small that they must consist only of one or a few molecular triglyceride layers. Evaluation of several cryoelectron micrographs

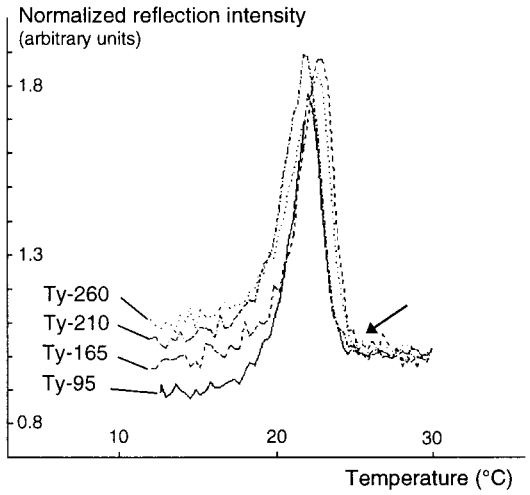

Figure 9. X-ray wide-angle reflection intensity in the region of the α-reflection (around 0.415 nm) of different D16 dispersions during the recrystallization process (cooling with 0.3125 °C/min). Prior to the onset of crystallization (arrow), the curves represent the diffuse scattering of the melt.

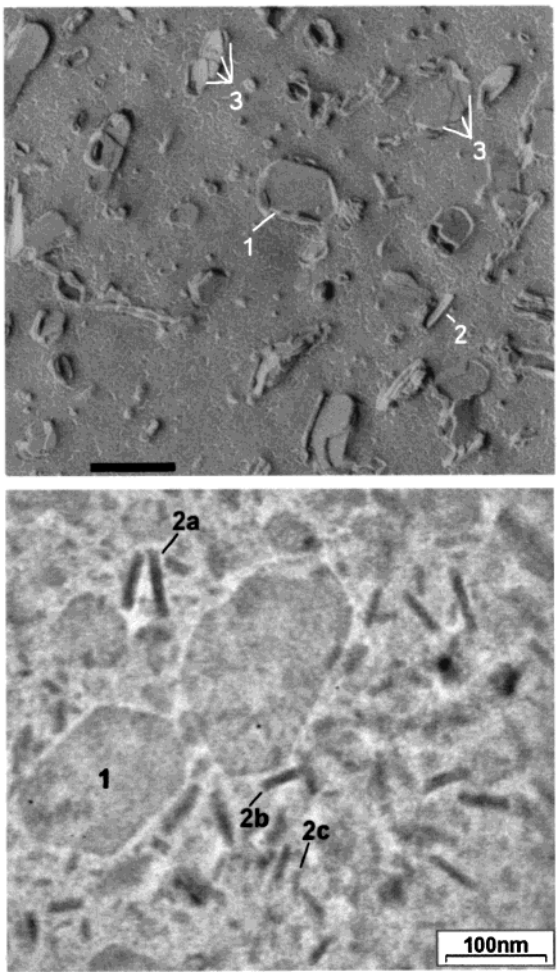

Figure 10. Electron micrograph of the freeze-fractured dispersion D16-Ty-165 (top, the bar corresponds to approximately 250 nm) and cryoelectron micrograph of the dispersion D16-Ty-100 (bottom). 1: Particle in top view. 2: Particle in side view (a ∼10, b ∼8, and c ∼5 nm thick). 3: Molecular layers.

of the dispersion D16-Ty-100 (corresponding to more than 100 particles with a suitable orientation) revealed particle thicknesses between approximately 5 and 20 nm (corresponding to about one to five molecular layers). Measurements on those particles are, however, not representative for the whole sample since cryoelectron microscopy allows only investigation of very thin aqueous films. Structures exceeding the thickness of the film cannot be or are only to a limited extent detected by this technique.

Discussion

The melting behavior of triglyceride nanoparticles strongly depends on particle size, irrespective of matrix material and stabilizer composition. From thermodynamics, it is expected that the melting temperature of colloidal substances would decrease with particle size,[11] and this has been observed with inorganic nanoparticles[12−15] and organic materials confined to nanoporous glasses.[16−18] Systematic studies on the melting behavior of suspension nanoparticles from crystalline organic substances have apparently not been performed so far.

Models based on the Thomson equation modified for crystalline materials or Gibbs−Thomson equation, respectively,

$$-\frac{T_0 - T}{T_0} \approx \ln\frac{T}{T_0} = -\frac{2\gamma_{sl}V_s}{r\Delta H_{fus}} \qquad (1)$$

are often used to describe the particle size dependence of the melting temperature[11,16] (where T is the melting temperature of a particle with radius r, T_0 is the melting temperature of the bulk material at the same external pressure, γ_{sl} is the interfacial tension at the solid−liquid interface, V_s is the specific volume of the solid, and ΔH_{fus} is the specific heat of fusion). It has been shown that this equation does not only apply for spherical (curved) particles but can also be used to describe the behavior of particles with plane surfaces.[11]

The Gibbs−Thomson equation has been used earlier to explain the melting point depression of triglyceride nanoparticles compared to their bulk phase.[3] For the size dependence of the melting point of inorganic nanoparticles, in particular, modified models are frequently used to account for deviations from the predicted linear relationship between relative melting point depression and particle curvature ($1/r$) frequently observed with such particles.[13,14,19,20] For materials confined to nanopores, inverse linear relations between T or ΔT and the pore size have, however, also been described.[16,17,21]

A shift of the melting transition to lower temperatures with decreasing mean particle size was also observed for the triglyceride suspensions under investigation. Since removal of large particles by ultracentrifugation was correlated with a decrease of the higher-melting fraction of the DSC curve, it can be concluded that in a given suspension the smaller particles melt at lower temperatures. This conclusion is supported by the fact that the line width of the small-angle X-ray reflections of smaller

(11) Defay, R.; Prigogine, I.; Bellemans, A.; Everett, D. H. *Surface Tension and Adsorption*; Longmans, Green & Co.: London, 1966; pp 243−244, pp 286−302.
(12) Takagi, M. *J. Phys. Soc. Jpn.* **1954**, *9*, 359−363.
(13) Buffat, P.; Borel, J.-P. *Phys. Rev. A* **1976**, *13*, 2287−2298.
(14) Allen, G. L.; Bayles, R. A.; Gile, W. W.; Jesser, W. A. *Thin Solid Films* **1986**, *144*, 297−308.
(15) Lai, S. L.; Guo, J. Y.; Petrov, V.; Ramanath, G.; Allen, L. H. *Phys. Rev. Lett.* **1996**, *77*, 99−102.
(16) Jackson, K. L.; McKenna, G. B. *J. Chem. Phys.* **1990**, *93*, 9002−9011.
(17) Mu, R.; Malhotra, V. M. *Phys. Rev. B* **1991**, *44*, 4296−4303.
(18) Unruh, K. M. *Nanostruct. Mater.* **1997**, *9*, 709−713.
(19) Coombes, C. J. *J. Phys. F* **1972**, *2*, 441−449.
(20) Couchman, P. R.; Jesser, W. A. *Nature* **1977**, *269*, 481−483.
(21) Unruh, K. M.; Huber, T. E.; Huber, C. A. *Phys. Rev. B* **1993**, *48*, 9021−9027.

size dispersions decreased during the melting process. The line width of a reflection is correlated with the number of repeating units in the crystal lattice underlying the reflection, i.e., with the size of the crystallites in the corresponding direction.

The course of the melting process of small-size triglyceride particles is very unusual. Except for H42, which displayed comparatively continuous DSC melting endotherms, all finely dispersed matrix materials exhibited a more or less stepwise melting event. None of the studies on the influence of particle size mentioned above describes a similar behavior, neither for inorganic nanoparticles nor for organic ones. Only for *n*-decane loaded into nanopores was a double DSC transition observed upon melting, but the effect was not investigated in further detail.[16]

The polymorphism of triglycerides is obviously not the cause of the stepwise melting process since no remarkable residues of metastable modifications could usually be detected. The particles thus melt from the stable β-form. For dispersions which, due to either their matrix structure (long chain triglycerides, complex triglyceride mixtures) or their stabilizer composition (phospholipid/sodium glycocholate blend), tend to transform comparatively slowly, the possibility of additional effects due to incomplete polymorphic transitions has, however, to be taken into consideration, in particular for freshly prepared systems.

Very finely dispersed systems displayed wide-angle X-ray reflections atypical of the stable β-modification of triglycerides. The structure underlying these reflections could be obtained in virtually pure form in ultracentrifugates retaining only particles with mean sizes between about 25 and 30 nm. The melting range of this structure is very low, approaching that of the α-modification in bulk. The structure of very fine particles thus differs significantly from that in the bulk or in coarser colloidal particles. This crystal structure seems to be unknown so far since its reflection pattern does not fit any of those reported in the classification of triglyceride polymorphs.[22] Similar reflections were detected for small triglyceride nanoparticles prepared by precipitation from solvent-in-water emulsions.[23] The special conditions in nanoparticles consisting only of one or a few molecular layers may influence the chain packing of the molecules and possibly also be responsible for the shift of the small-angle reflection.

The existence of only one additional, low-melting structure in very fine particles is, however, not sufficient to explain the complex melting behavior of the dispersions at higher temperatures. According to the X-ray measurements, the complex melting behavior must be due to a stepwise melting of the stable β-form. For the β-modification of triglycerides, several submodifications which differ in angle of chain tilt and thus in their long spacings have been described.[24,25] It is, however, unlikely that the complex melting behavior of triglyceride nanoparticles is caused by the successive melting of these submodifications since there were only minor changes in the position of the small-angle reflection during melting (Figure 8). The structure underlying the peak shoulder to larger angles in some diffractograms of very fine dispersions (which, according to its position in the diffractogram, might be caused by the presence of the β_{IV} or β-2E submodification) does not seem to be the cause of the complex melting event, either, since it was present until the end of the transition.

Consequently, the stepwise melting event is most probably due to the particular crystal shape and the layered structure of the triglyceride nanoparticles. The particle shape is similar to that of triglyceride single crystals in which the molecular triglyceride layers are positioned parallel to the large (001) faces. The smallest colloidal dimension of the nanoparticles, the platelet height, can only take on discrete values which are multiples of the triglyceride layer thickness (disregarding the emulsifier layer). Because of the length of the triglyceride chains, the differences in possible platelet heights are of colloidal size, and at least for thin particles, cannot be neglected in relation to the overall platelet height. By assuming that the relation γ_{sl}/r in the Gibbs−Thomson equation for crystals is more precisely expressed by γ_x/r_x where the relative dimensions of a crystal in equilibrium are interrelated via the interfacial tensions γ_x of the corresponding crystal faces by[11]

$$\frac{\gamma_x}{r_x} = \frac{\gamma_1}{r_1} = \frac{\gamma_2}{r_2} = \frac{\gamma_3}{r_3} = \text{const.} \qquad (2)$$

half of the height of a nanocrystal may be used as the size parameter in the Gibbs−Thomson equation (where γ_x is the interfacial tension of the surface x and r_x is the distance between the crystal surface x and the center of the crystal). Since the height of the triglyceride nanoparticles can only change in steps corresponding to the thickness of the single triglyceride layers (reflected by the d_{001} value), this will result in distinct melting temperatures reflecting the differences in particle height. Each of the individual transitions observed in the melting event would thus be due to the melting of a class of particles with a well-defined platelet height. Recent results obtained from line-shape analysis of X-ray reflections arising from triglyceride suspensions during the melting process support this conclusion.[26]

To estimate the magnitude of the effect on the melting temperature to be expected from the stepwise increase in particle thickness, model calculations assuming particles with different heights and values for the interfacial tension were performed. These calculations yielded values of melting temperatures changing in steps that are of the same order as those obtained experimentally (Figure 11). The experimental values do not, however, reflect the succession of melting temperatures derived from the model calculations but this may be due to oversimplification of the model. The model calculation is based inter alia on the assumption that except for the particle size all quantities in the Gibbs−Thomson equation are constant. This assumption is not valid for the heat of fusion, for instance, which usually decreased with the mean size of the triglyceride suspensions in agreement with experimental results on other systems.[15−18,21] A general expression describing the relation between particle size and heat of fusion or corresponding experimental data for triglyceride nanoparticles is, so far, not available. On the basis of the present data, it thus does not seem promising to fit the experimental results to a theoretical model, in particular since other parameters of the equation (specific volume, interfacial tension) might also depend on particle size. Moreover, the contribution of the additional low melting structure is difficult to evaluate.

(22) Hoerr, C. W.; Paulicka, F. R. *J. Am. Oil Chem. Soc.* **1968**, *45*, 793−797.
(23) Siekmann, B.; Westesen, K. *Eur. J. Pharm. Biopharm.* **1996**, *43*, 104−109.
(24) Frede, E.; Precht, D. *Fette Seifen Anstrichm.* **1977**, *79*, 69−75.
(25) de Jong, S.; van Soest, T. *Acta Crystallogr. B* **1978**, *34*, 1570−1583.
(26) Unruh, T.; Bunjes, H.; Westesen, K.; Koch, M. H. J. *J. Phys. Chem. B* **1999**, 10373−10377.

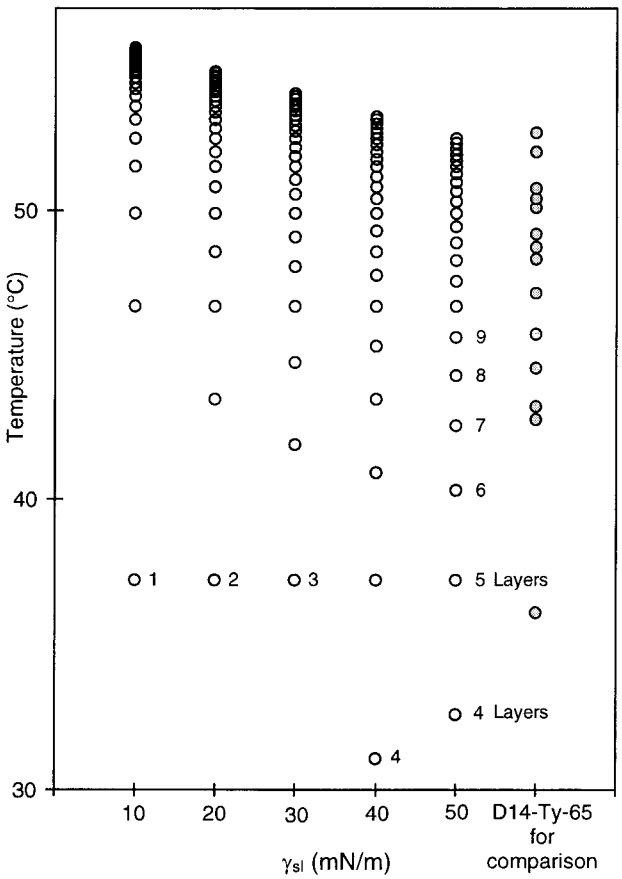

Figure 11. Melting temperatures of the dispersion D14-Ty-65 (Micro DSC III, 0.04 °C/min) and transition temperatures of trimyristin calculated on the basis of the Gibbs−Thomson equation in dependence on interfacial tension γ_{sl} and the number of molecular triglyceride layers (given are the values for consecutive layers beginning with the values given in the diagram) using the following values: T_0: 56.4 °C; V_s: 0.980 cm^3/g; ΔH: 178 J/g; d_{001} (trimyristin): 3.59 nm. The emulsifier layer was neglected for the model calculation.

The loss of structuring of the melting process with increasing complexity of the matrix triglyceride may have several causes. In all likelihood, a single particle consisting of a complex triglyceride will melt over a larger temperature range than a particle of a simple triglyceride. Moreover, the height of nanocrystals obtained from complex triglycerides is not necessarily an exact multiple of the average triglyceride layer thickness (obtainable from the X-ray spacings) since the composition of the nanocrystal and thus also the thickness of the single molecular layers may not be homogeneous. The broad pretransitions in H42 dispersions could result from particle size effects as well as from the existence of metastable modifications since, particularly with small size dispersions, a partial melting can hardly be avoided during sample preparation.

It cannot completely be excluded that other effects contribute to the particle size effect. Although there were no indications for significant interactions between tyloxapol and D16 in bulk mixtures (data not shown) some interaction of surfactant and matrix material at the particle surface may still be possible at the colloidal level. Such "surface contamination" of the matrix material was considered the cause for a "premelting" effect in dispersed hexane.[27] A gradual melting of single particles as assumed for the hexane particles can, however, be ruled out for triglyceride nanoparticles on the basis of the experimental results. A gradual, layer- or surfacewise melting of single particles would be expected to result in a broadening of the X-ray reflections upon heating instead of the observed sharpening of the small-angle reflection. Moreover, the crystallinity of partially melted particles should increase following a slight decrease in temperature. The crystallization temperature of the nanoparticles in a sample containing only a fraction of its D16 content in the melted state was, however, comparable to that in a nanodispersion of completely melted D16.

The influence of particle size on crystallization is far less pronounced than that on melting. Compared to the overall depression of the crystallization temperatures with respect to the bulk material,[4] the differences in the particle size range under investigation are small. The rate of polymorphic transitions after crystallization increases with decreasing particle size. The relaxation of the lattice strain developing during the transition may be facilitated in smaller crystalline particles due to their higher specific surface area or small particles may more readily provide the energy of activation required for the transition as a result of their higher energy level.[28,29]

Conclusions

The melting behavior of triglyceride nanoparticles strongly depends on particle size. Monoacid triglyceride particles in the lower colloidal size range display an uncommon, stepwise melting process which is correlated with the thickness distribution of the plateletlike particles: Each fraction of particles with the same number of molecular layers melts within a small, defined temperature range. As a result, a sequence of discrete melting events is observed for the dispersion as a whole. Moreover, the triglycerides in very small particles crystallize in a form which has hitherto not been described.

To evaluate the general character of the effect observed in the present study, further investigations on organic, in particular, long-chain compounds are required. Studies on fractionated dispersions might help to develop a more detailed theoretical approach and to obtain further information on the crystalline structure present in very small-size colloidal dispersions.

Acknowledgment. The authors thank M. Drechsler, S. Richter, D. E. Lesemann, C. Gröchtemeyer, and A. Gerke for their contributions to the electron microscopic investigations, and S. Liedtke for assistance in sample preparation.

LA990856L

(27) McClements, D. J.; Dungan, S. R.; German, J. B.; Kinsella, J. E. *Colloids Surf. A* **1993**, *81*, 203-210.
(28) Dafler, J. R. *J. Am. Oil Chem. Soc.* **1977**, *54*, 249−254.
(29) Whittam, J. H.; Rosano, H. L. *J. Am. Oil Chem. Soc.* **1975**, *52*, 128−133.